

# SIMULATION OF SUNSPOT ACTIVITY DURING ACTIVE SUN AND GREAT MINIMA USING REGULAR, RANDOM AND RELIC FIELDS

I. G. USOSKIN<sup>1,\*</sup>, K. MURSULA<sup>2</sup> and G. A. KOVALTSOV<sup>3</sup>

<sup>1</sup>*Sodankylä Geophysical Observatory (Oulu unit), FIN-90014 University of Oulu, Finland*

<sup>2</sup>*Department of Physical Sciences, FIN-90014 University of Oulu, Finland*

<sup>3</sup>*Ioffe Physical-Technical Institute, 194021 St. Petersburg, Russia*

(Received 15 September 2000; accepted 31 October 2000)

**Abstract.** Developing the idea of Ruzmaikin (1997, 1998), we have constructed a model of sunspot production using three components of solar magnetic field: the 22-year dynamo field, a weak constant relic field, and a random field. This model can reproduce the main features of sunspot activity throughout the 400-year period of direct solar observations, including two different sunspot activity modes, the present, normal sunspot activity and the Maunder minimum. The two sunspot activity modes could be modeled by only changing the level of the dynamo field while keeping the other two components constant. We discuss the role of the three components and how their relative importance changes between normal activity and great minimum times. We found that the relic field must be about 3–10% of the dynamo field in normal activity times. Also, we find that the dynamo field during the Maunder minimum was small but non-zero, being suppressed typically by an order of magnitude with respect to its value during normal activity times.

## 1. Introduction

Time evolution of sunspot activity (SA) is of great interest for solar physics since it reflects processes in the solar convection zone. The main feature of SA is its 11-year cycle due to the action of the dynamo mechanism. The 11-year cyclicity is modulated by long-term effects, such as the secular Gleissberg cycle (for a review see, e.g., Wilson, 1994; Vitinsky, 1965; Vitinsky, Kopecký, and Kuklin, 1986). Sometimes sunspot activity is dramatically suppressed, leading to a so-called great minimum. The most recent great minimum was the Maunder minimum (MM) in 1645–1715 when sunspot activity almost vanished (Eddy, 1976).

Earlier it was common to describe SA as a multi-harmonic process with several fundamental harmonics superposed with each other (see, e.g., Sonett, 1983; Vitinsky, 1965; Vitinsky, Kopecký, and Kuklin, 1986). On the other hand, SA series also contains a random component which is larger, e.g., than the observational uncertainties. Since the early 1990s, several authors have studied solar activity as an example of low-dimensional deterministic chaos described by a strange attractor (see, e.g., Ostryakov and Usoskin, 1990; Mundt, Maguire, and Chase, 1991; Rozelot, 1995). This approach has been criticized because the analyzed data set is

\*On leave from Ioffe Physical Technical Institute, 194021 St. Petersburg, Russia.



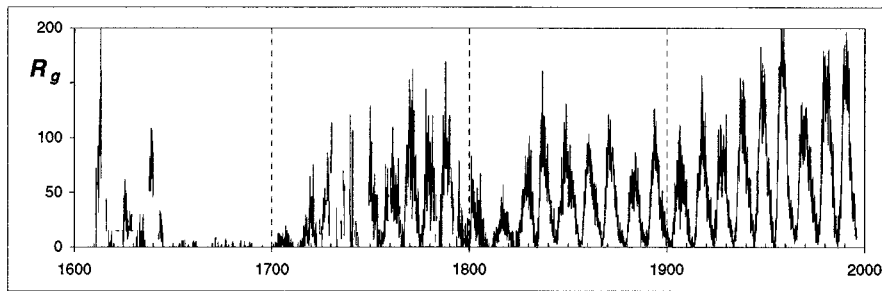


Figure 1. Monthly group sunspot numbers.

too short (Carbonell, Oliver, and Ballester, 1993, 1994) and disturbed by filtering (Price, Prichard, and Hogenson, 1992). While the majority of earlier studies have concentrated on either the regular or the random component of SA, some studies have included both components (e.g., Sonett, 1982; Ruzmaikin, 1997, 1998). However, only the normal sunspot activity level is studied in these papers. On the other hand, it has been suggested that the dynamo can be in a quite different mode during the great minima than during times of normal SA level (see, e.g., Sokoloff and Nesme-Ribes, 1994; Schmitt, Schüssler, and Ferriz-Mas, 1996, and references therein). Correspondingly, the relation between the regular and random components of SA can be very different during great minima and normal activity times.

In this paper we present a unified model of sunspot production during the two different modes of sunspot activity level. The magnetic field in the bottom of the convection zone is considered to be a superposition of a regular and a random component, and sunspots are produced if this total field exceeds a buoyancy threshold (Ruzmaikin, 1997, 1998). In addition to the normal dynamo field, the regular component in our model also includes a constant magnetic field, corresponding to the relic solar magnetic field (Cowling, 1945; Sonett, 1982; Levy and Boyer, 1982; Pudovkin and Benevolenskaya, 1984) recently found in the persistent 22-year cyclicity in SA (Mursula, Usoskin, and Kovaltsov, 2001). The relic field can, due to the amplification by the dynamo mechanism, play a significant role in sunspot occurrence (Levy and Boyer, 1982; Boyer and Levy, 1984; Boruta, 1996). Our model can reproduce the main features of SA both during great minima and normal activity times. In Section 2 we review the basic features of SA during the Maunder minimum and normal activity times. In Section 3 we describe the details of the model and simulations. Section 4 presents the simulation results and Section 5 discuss the results obtained. In the final Section 6 we present our conclusions.

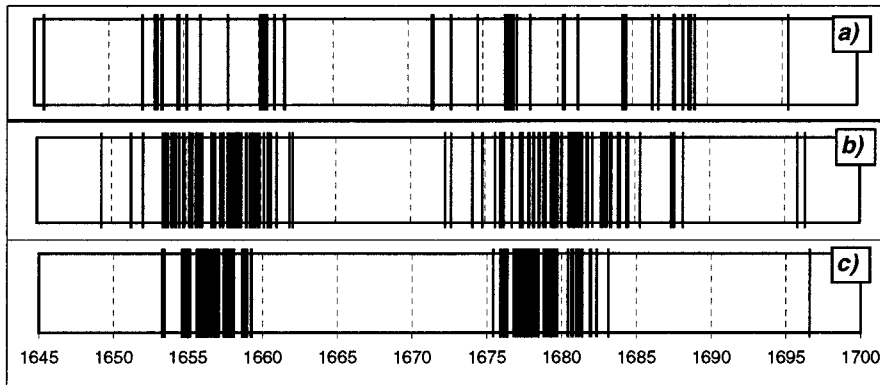


Figure 2. Days with sunspots during the deep Maunder minimum. (a) Actual observations according to the GSN series. (b) A sample of simulation for case I with  $B_0 = 0.05$ ,  $\sigma_0 = 3$ ,  $A_{11} = 0.05$ . (c) A sample of simulation for case II with  $B_0 = 0.05$ ,  $\sigma_0 = 3$ ,  $A_{11} = 0.1$

## 2. Properties of Sunspot Activity

As the SA index we use the new group sunspot number (GSN) series (Hoyt and Schatten, 1998) which covers the period since 1610 and, thus, includes the full MM period. Moreover, this series is a more correct and homogeneous SA proxy for the period before 1850 than the Wolf number series (Hoyt and Schatten, 1998; Wilson, 1998; Letfus, 1999). The monthly GSN series is shown in Figure 1. As seen there, the behavior of SA during MM was significantly different from that during the rest of the interval covered by GSN series which depicts a clear 11-year cyclicity.

### 2.1. MAUNDER MINIMUM

During the Maunder minimum more than 95% of days were covered with sunspot observations (Hoyt and Schatten, 1996). However, sunspots were registered in less than 2% of days during that period. Because of the sparse and seemingly sporadic occurrence of sunspots, traditional methods of time series analysis are not appropriate for this period (Frick *et al.*, 1997; Mordvinov and Kuklin, 1999). Recently we performed, using a special method, a detailed study of sunspot occurrence during MM (Usoskin, Mursula, and Kovaltsov, 2000). Since the exact daily GSN values are small and not very accurate during MM (Hoyt and Schatten, 1996), we only used the information whether a sunspot was reported for a certain day or not. Days with observed sunspots during the deep MM in 1645–1700 are shown in Figure 2(a) as vertical bars. As discussed in more detail by Usoskin, Mursula, and Kovaltsov (2001), sunspot occurrence was grouped into two major intervals, (1652–1662) and (1672–1689), with a high statistical significance. The ‘mass centers’ of these intervals were in 1658 and 1679–1680, respectively. These mass centers together with the first SA maximum after the deep MM (1705) and the last maximum before MM (1639–1640) imply a roughly 22-year variation of SA during

MM (Usoskin, Mursula, and Kovaltsov, 2001). (Despite this dominant feature, a sub-dominant 11-year cycle in SA may have existed, especially in the second half of MM (see also Nesme-Ribes, 1993).)

Thus, we can summarize the two main features of SA during the deep MM as follows:

(1) Sunspots occurred seldom, approximately on 2% of days.

(2) Daily sunspot occurrence was grouped into two long intervals, in 1652–1662 and 1672–1689, with hardly any activity outside these intervals in 1645–1652, 1662–1672, and 1689–1699.

## 2.2. NORMAL SOLAR ACTIVITY

The main feature of SA during normal activity times is the 11-year Schwabe cycle. One important parameter of SA during these times is the ratio between SA maxima and minima attained during one cycle. Using the standard 12-month running average, one can find that this maximum to minimum ratio in the GSN series varies from about 10 to 200 for the solar cycles after the Dalton minimum in the beginning of the 19th century.

Recently we have shown (Mursula, Usoskin, and Kovaltsov, 2001) that a persistent 22-year cyclicity exists in SA with a roughly constant amplitude of about 10% of the modern SA level. This 22-year cyclicity is the underlying feature behind the well-known empirical Gnevyshev–Ohl (G–O) rule (Gnevyshev and Ohl, 1948; Wilson, 1988; Storini and Šýkora, 1997) according to which the sum of sunspot numbers over an odd cycle exceeds that of the preceding even cycle. The 22-year cyclicity in sunspot activity is naturally explained by the action of the 22-year solar dynamo cycle in the presence of a weak solar relic field (see Mursula, Usoskin, and Kovaltsov, 2001, and references therein).

In order to study the random component of SA during normal SA level, we first removed the 31-month running average,  $\langle R \rangle_i$ , from the raw monthly GSN series,  $R_i$ . The residual  $R_i - \langle R \rangle_i$  has a significantly asymmetric distribution, in agreement with the fact that the noise in SA series is ‘colored’ or correlated (e.g., Oliver and Ballester, 1996; Frick *et al.*, 1997; Ruzmaikin, 1998), i.e., the variance of the noise depends on the current level of SA. Therefore, we study the normalized residual:

$$r_i = \frac{R_i - \langle R \rangle_i}{\langle R \rangle_i} . \quad (1)$$

The normalized residual is shown in Figure 3(a) for 1849–1996. Figure 3(b) shows the histogram of this normalized residual. While the distribution is nearly Gaussian around zero, there are some side effects in the distribution at  $|r_i| > 0.8$ . The wings of the distribution are not symmetric since  $r_i \geq -1$  by definition (Equation (1)) while there is no upper limit for  $r_i$ . Moreover, values of  $R_i = 0$  are over-represented in SA, especially around SA minima, leading to enhanced probability of  $r_i \approx -1$  with respect to the Gaussian shape and to the small negative mean of the distribution. The fit of the histogram distribution in the range of  $[-0.9; 0.9]$  by a Gaussian

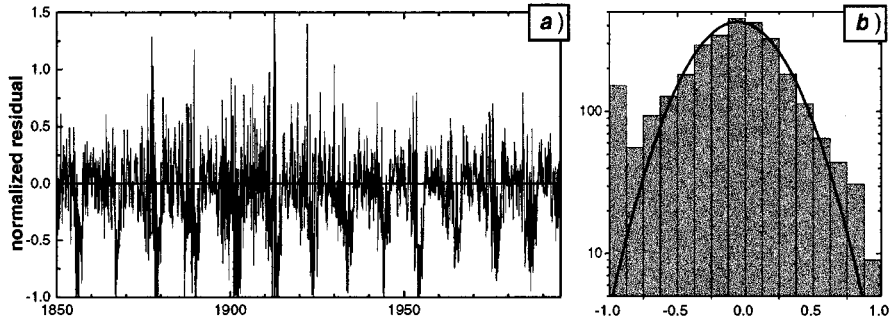


Figure 3. (a) The normalized residual between the raw and smoothed monthly GSN series for the period 1849–1996. (b) Distribution of the residual with the best fit Gaussian (mean =  $-0.05$ , standard deviation  $\approx 0.3$ ).

curve yields the mean of  $-0.05$  and the standard deviation of about  $0.3$ . The  $\chi^2$ -test suggests that the distribution is Gaussian with the significance level of 78% ( $\chi_6^2 = 3.2$ ).

Thus, we can summarize the three main features of SA during normal activity times as follows:

- (1) The 11-year SA cycle is the dominant feature. The ratio between the 12-month smoothed sunspot maxima and minima during one cycle is 10–200.
- (2) There is a persistent, roughly constant 22-year cycle in sunspot activity at about a 10% level of the present SA.
- (3) Monthly GSN values fluctuate randomly around the running average forming a correlated noise. The normalized noise has nearly Gaussian distribution.

### 3. The Simulation Model

Following Ruzmaikin (1997, 1998), we adopt the condition that if the total magnetic field in the dynamo layer of the convection zone exceeds a buoyancy threshold, sunspots will occur. Ruzmaikin (1997) considered the total field consisting of two parts:

$$B_{\text{tot}} = B_{\text{reg}} + b, \quad (2)$$

where the regular  $B_{\text{reg}}$  field only includes the 11-year oscillating, dynamo-related field  $B_{11}$ , and  $b$  is the randomly fluctuating field generated by random motions (Ruzmaikin, 1998, and references therein). While the buoyancy threshold at the bottom of the convection zone is supposed to be about  $10^5$  G (see, e.g., Schüssler *et al.*, 1994; Caligari, Moreno-Inertis, and Schüssler, 1995), estimates of the mean field in that region vary from  $10^4$  to  $\leq 10^5$  G (e.g., Zeldovich, Ruzmaikin, and Sokoloff, 1983; Schüssler *et al.*, 1994; Ruzmaikin, 1998). This implies that the regular field in the mean-field  $\alpha - \Omega$  dynamo theories is below the threshold, and therefore the random  $b$ -field is important in order to exceed the threshold.

In view of including the relic field in our model, we have to retain the direction of the  $B_{11}$  field. Therefore we take the  $B_{11}$  field in the form of a 22-year sinusoid (Hale cycle) with amplitude  $A_{11}$  (e.g., Sonett, 1982; Bracewell, 1986):

$$B_{11}(t) = A_{11} \sin(\pi t / T_{11}), \quad (3)$$

where  $T_{11} = 11$  years. Accordingly, the regular magnetic field in our model is

$$B_{\text{reg}} = B_{11} + B_0, \quad (4)$$

where  $B_0$  is the constant relic magnetic field.

We have used the two different types of randomly fluctuating field appearing in literature with different probability distribution functions  $p(b)$ . Ruzmaikin (1998) suggested that the distribution function of the solar random field might have an exponential tail:

$$p(b) \sim \exp\left(\frac{-|b|}{\sigma}\right). \quad (5)$$

However, usually, the normal (Gaussian) distribution of random values is used when modeling physical processes (see, e.g., Sonett, 1983):

$$p(b) \sim \exp\left(\frac{-b^2}{2\sigma^2}\right). \quad (6)$$

Since arguments have been given in favor of both models, we will use both distributions in our simulations, calling them case I (exponential distribution) and case II (Gaussian distribution), respectively. Since the random component of SA is due to correlated noise, the variance of the noise  $\sigma(t)$  is assumed to be proportional to the regular component of the field at each time (Ostryakov and Usoskin, 1990a):

$$\sigma(t) = \sigma_o |B_{\text{reg}}(t)|, \quad (7)$$

where  $B_{\text{reg}}$  is given according to Equation (4). We also note that since the random field can attain both negative and positive values in our model, the corresponding distribution functions are normalized to one from minus to plus infinity.

#### 4. Simulation Results

Using Equations (2)–(7), we numerically simulated SA separately for normal solar activity and for the great minimum. For each day  $t$ , the value of the random field  $b$  was generated by a pseudo-random number generator having either the exponential (Equation (5)) or the Gaussian (Equation (6)) distribution with  $\sigma(t)$  defined by Equation (7). Adding the  $b$ -field to the corresponding regular field component, the total  $B_{\text{tot}}$  for one day was obtained (Ruzmaikin, 1997). The absolute value of the simulated total field,  $|B_{\text{tot}}|$ , was then compared with the threshold  $B_{th}$ . If the total

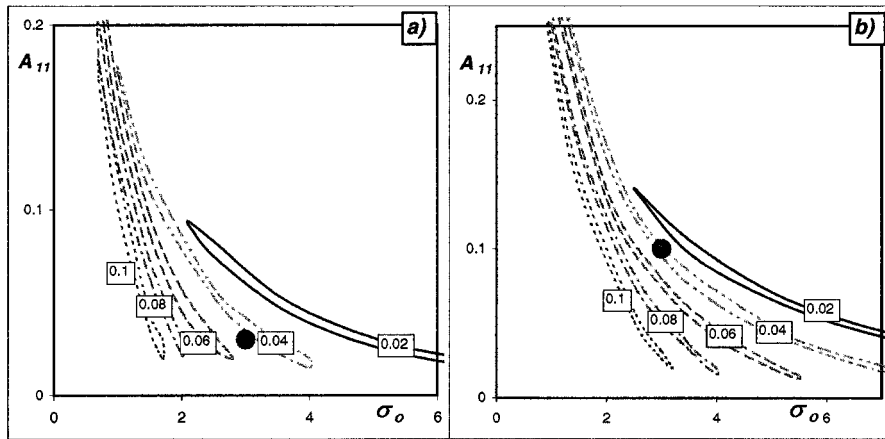


Figure 4. Area of possible values of model parameters  $A_{11}$  vs.  $\sigma_0$  for the Maunder minimum. Value of  $B_0$  is fixed (as shown in boxes). (a) and (b) are for case I and case II, respectively. Big solid circles denote values of parameters used for sample simulations shown in Figure 2.

field exceeded the threshold, sunspots occurred on that day, and the daily sunspot number was proportional to  $(|B_{\text{tot}}| - B_{\text{th}})$ . Field values are in arbitrary units with the value of the threshold,  $B_{\text{th}}$ , chosen to be unity. Accordingly, there are three independent parameters in the model:  $A_{11}$ ,  $B_0$ , and  $\sigma_0$ .

#### 4.1. THE DEEP MAUNDER MINIMUM

During the deep MM, the 11-year SA cycle is found to be very weak (see Section 2.1). Accordingly, we assume that  $A_{11}$  was small (but non-zero) during this time. A sample of simulated sunspot occurrence is shown in Figure 2(b) for case I and in Figure 2(c) for case II. These samples show a time behavior which is rather similar to that of the actual sunspot occurrence. We have made  $10^4$  simulation sets of 20088 days (simulations) each, corresponding to the number of days in the deep MM in 1645–1699.

In the following we try to find the range of the three model parameters which satisfies the two main features of SA during the deep MM (see Section 2.1), now given as the following two constraints:

Constraint I. There were 369 sunspot days out of the 20088 days of the deep MM. The number of simulated sunspot days was constrained to be  $369 \pm 57$  (99.7% confidence level).

Constraint II. There were long spotless periods in 1645–1652, 1662–1672, and 1690–1699 (see Figure 2(a)). We require that the sunspot occurrence rate during the long spotless periods in 1645–1652, 1662–1672, and 1690–1699 (see Figure 2(a)) is significantly lower (with significance level higher than 99.9%) than during other periods of the deep MM. Not more than one sunspot day per year is allowed in these intervals.

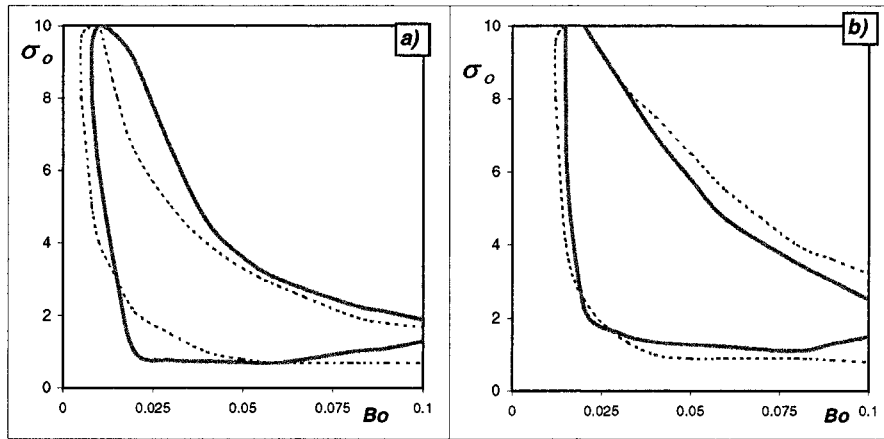


Figure 5. Area of possible values of model parameters  $\sigma_0$  vs.  $B_0$  for case I and case II (panels (a) and (b)), respectively. The allowed area of the parameter values is limited by the *solid curve* for the normal SA times, and by the *dotted curve* for the Maunder minimum.

Using these constraints we found areas of model parameter values which are shown in Figures 4(a) and 5(a) for case I and in Figures 4(b) and 5(b) for case II. Figure 4 presents the relationship between the amplitude  $A_{11}$  and the  $\sigma_0$  parameter for several values of the relic field  $B_0$ . One can see that, for a fixed  $B_0$ , the allowed area is prolonged and very narrow in both cases, reflecting the approximate inverse relation between the two parameters. This is mainly due to the effect of constraint I. The area of the possible values of  $\sigma_0$  and  $B_0$  (irrespective of the value of  $A_{11}$ ) is limited by the two dotted lines in Figure 5.

#### 4.2. NORMAL SUNSPOT ACTIVITY TIMES

Some samples of simulated SA for normal activity times are shown in Figures 6(b) and 6(c) for case I and case II, respectively. There is a good overall similarity with the actual GSN data (Figure 6(a)) for the period of fairly constant SA level (solar cycles 9–13). Contrary to real cycles, the simulated cycles are symmetric since we assumed a sinusoidal shape for the underlying 11-year cycle (Equation (3)). We simulated 1000 11-year solar cycles for each of the two cases. The length of simulated cycles varied from 9.5 to 12.5 years, and the cycle amplitude changed by a factor of two, in good agreement with the real sunspot cycles. In accordance with the observed 22-year variation, the G–O rule was found to be valid throughout the entire simulated series.

Next we try to find the parameter range which satisfies the three main features of SA during normal activity times (Section 2.2.) which are now given as the following two constraints:

Constraint I (feature 1 of Section 2.2) limits the ratio of the (12-month averaged) sunspot maxima and minima of a cycle to within 10–200.

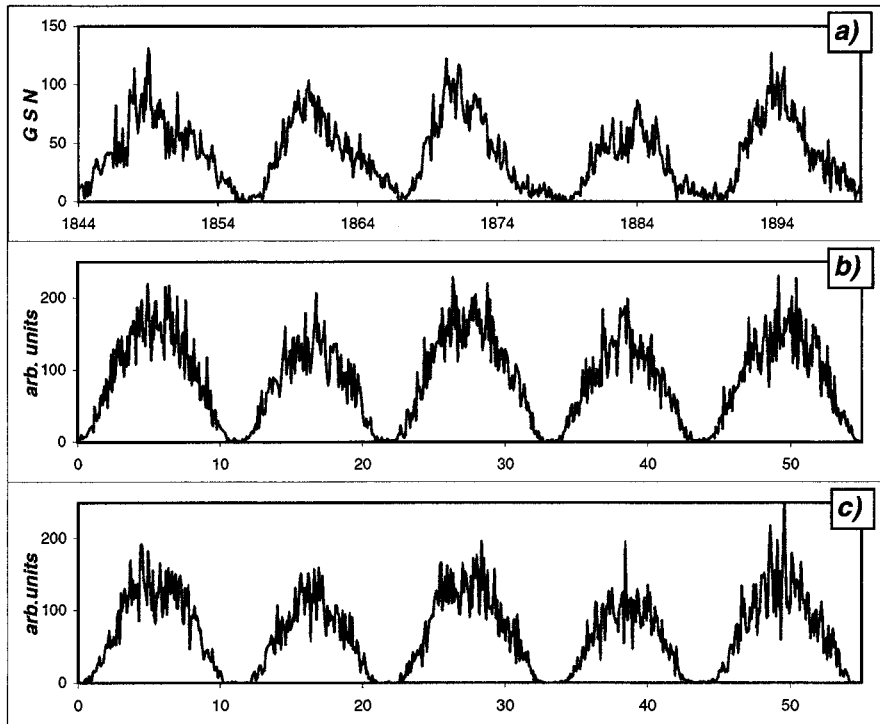


Figure 6. Sunspot activity: (a) actual monthly group sunspot numbers for the period of roughly constant SA level; (b) a sample of the monthly simulated SA for case I with  $A_{11} = 0.6$ ,  $B_0 = 0.05$ ,  $\sigma_0 = 3$ ; (c) a sample of the monthly simulated SA for case II with  $A_{11} = 0.7$ ,  $B_0 = 0.05$ ,  $\sigma_0 = 0.3$ .

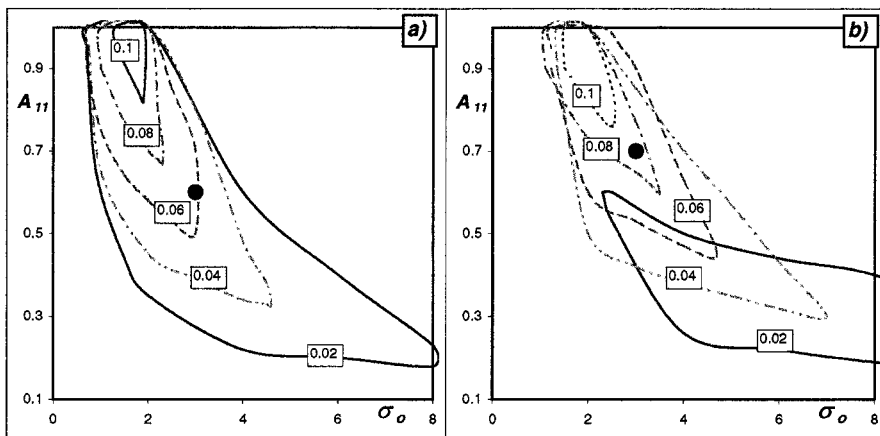


Figure 7. Area of possible values of model parameters  $A_{11}$  vs.  $\sigma_0$  for the normal sunspot activity times. Value of  $B_0$  is fixed (as shown in boxes). (a) and (b) are for case I and case II, respectively. *Big dots* denote values of parameters used for sample simulations shown in Figure 6.

Constraint II (feature 3 of Section 2.2) requires that the odd cycles are 10–30% more intense than even cycles. Note that the ratio between the 22-year variation in cycle intensity and the average intensity level is about  $20\% \pm 10\%$  (Mursula, Usoskin, and Kovaltsov, 2001).

Feature 2 of Section 2.2 was not a constraint but rather was adopted within the method. (See discussion later in this section). The relation between  $A_{11}$  and  $\sigma_0$  for fixed  $B_0$  is shown in Figures 7(a) and 7(b) for case I and case II, respectively. The two parameters are in rough inverse relation, in analogy with the results for the deep MM period (see Figure 4). However, the area is now wider because no constraint was given to the SA cycle amplitude, contrary to MM. The area of the possible values of  $\sigma_0$  and  $B_0$  (irrespective of the value of  $A_{11}$ ) is limited by the two solid lines in Figure 5.

Finally, we smoothed the simulated sunspot series and studied the monthly residual in the same way as done in Section 2.2. The normalized residuals for samples shown in Figures 6(b) and 6(c) appear to have a Gaussian shape for both case I and case II with roughly zero means ( $-0.03$  and  $-0.02$ ) and standard deviations of about 0.26 and 0.25, respectively. These parameters are close to those obtained for the actual GSN series.

## 5. Discussion

As seen in Figures 2 and 6, our model can reproduce the time evolution of SA during both great minima and normal activity times. The range of possible values of  $B_0$  and  $\sigma_0$  (Figure 5) is essentially similar for these two very different modes of SA. It is important to note that the model can reproduce SA behavior for the two modes with the same values of  $B_0$  and  $\sigma_0$ , only changing the amplitude of the 11-year cycle. This implies that the dynamo can be significantly suppressed during great minima while both the relic field and random component remain constant. Figure 5 also shows that the value of  $\sigma_0$  must be larger than about one in both cases. This corresponds to the fact that the fluctuating field is necessary in order to exceed the buoyancy threshold within the assumption of a regular field being below the threshold (see Section 3).

We note that both the exponential (case I) and the Gaussian (case II) distributions of the fluctuating field can reproduce the time behavior of SA. Moreover, areas of possible values of model parameters are very similar for the two cases in both modes of sunspot activity (compare panels (a) and (b) in Figures 4, 5, and 7). However, the exponential distribution may be slightly more suitable for MM since it produces a wider spread of sunspot days around the 22-year maxima, in better accordance with observations (see Figure 2). The fact that measures of randomness of the simulated series are similar to those of the actual GSN data, suggests that we have correctly simulated the fluctuating field.

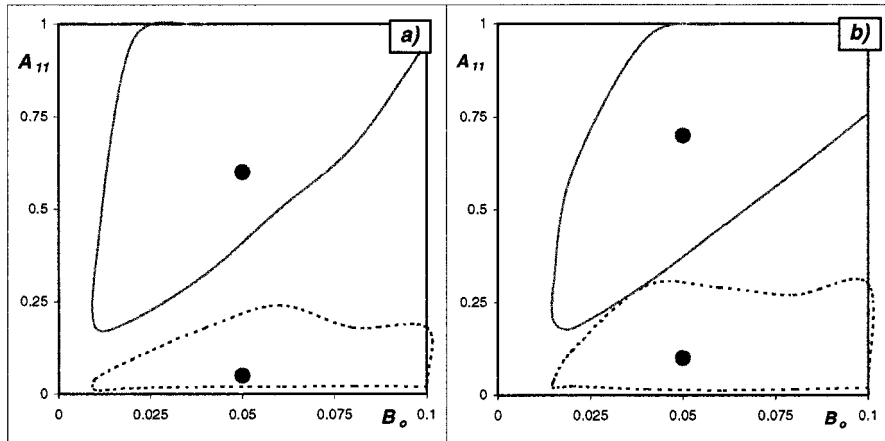


Figure 8. Area of possible values of model parameters  $A_{11}$  vs.  $B_0$  for cases I and II ((a) and (b)), respectively. The allowed area of the parameter values is limited by the *solid curve* for the normal SA times, and by the *dotted curve* for the Maunder minimum. *Big solid circles* denote parameters used for sample simulations in Figures 2 and 6.

We found in Figure 7 that the relic field is constrained to be roughly below 0.1 within the model assumptions. In order to better study the range of allowed values of  $B_0$  we have shown the relation between  $A_{11}$  and  $B_0$  in Figure 8. We can see that there is a lower limit for  $B_0$  of about 0.01 in case I and 0.015 in case II. We note that a lower limit of the same order of magnitude is found from constraints of both modes of sunspot activity. Accordingly, the existence of the relic field is necessary in both modes of SA in order to satisfy the model constraints. Since the constraints are based on rigorous observational facts, this result gives further evidence for the existence of the relic field. Moreover, we obtain a new estimate for the magnitude of the relic field of about 1–10% of the threshold field. It is also interesting to note that the two cases of random field yield a roughly similar range for the value of the relic field.

Figure 8 also shows that the amplitude of the dynamo field,  $A_{11}$ , can not be less than about 20% of the threshold during normal SA times. We also find that the value of  $A_{11}$  during MM is limited to within 0.02–0.2 in case I and 0.02–0.3 in case II. The fact that the areas of possible parameters in Figure 8 for the two modes of SA do not overlap implies that the dynamo was really in different modes during MM and in ‘normal’ SA times. The lower limit on  $A_{11}$  during MM implies that the dynamo has to operate at some level even during the lowest sunspot activity times. However, it was suppressed during the deep MM by typically a factor of 10–30 with respect to the normal SA mode. Also, according to Figure 8, the upper bound on the relic field amplitude  $B_0$  is roughly linearly dependent on the value of  $A_{11}$  for normal activity times being roughly 10% of the dynamo field.

## 6. Conclusions

We have shown that the main features of sunspot activity throughout the entire period of direct solar observations, including two different sunspot activity modes ('normal' sunspot activity and great minimum times), can be reproduced by a simple model consisting of the 22-year dynamo field, a weak constant relic field and a random field. The two SA modes could be modeled by only changing the level of the dynamo field while keeping the other two parameters (relic field amplitude and variance of random field) constant. We have studied the role of the three components in sunspot production and discussed how their relative importance changes between normal activity times and great minima. We found that, in order to explain the observed level of 22-year cyclicity in sunspot activity (Mursula, Usoskin, and Kovaltsov, 2001), the relic field must be about 3–10% of the dynamo field in normal SA times. The possibility of such a relic field was first shown theoretically by Cowling (1945), then discussed, e.g., by Sonett (1982), Levy and Boyer (1982), Pudovkin and Benevolenskaya (1984), Bravo and Stewart (1995), and Boruta (1996). Also, we find that the dynamo field during the Maunder minimum was small but non-zero, being suppressed typically by an order of magnitude with respect to its value during normal activity times. Moreover, we note that the obtained results are only slightly different between the two assumptions on the nature of the random field.

## Acknowledgements

We gratefully thank the Academy of Finland for financial support. The *ftp* service of NOAA is appreciated for an easy access to the GSN data.

## References

- Bracewell, R. N.: 1986, *Nature* **323**, 516.  
Bravo, S. and Stewart, G.: 1995, *Astrophys. J.* **446**, 431.  
Boruta, N.: 1996, *Astrophys. J.* **458**, 832.  
Boyer, D. W. and Levy, E. H.: 1984, *Astrophys. J.* **277**, 848.  
Caligari, P., Moreno-Insertis, F., and Schüssler, M.: 1995, *Astrophys. J.* **265**, 1056.  
Carbonell, M., Oliver, R., and Ballester, J. L.: 1993, *Astron. Astrophys.* **274**, 497.  
Carbonell, M., Oliver, R., and Ballester, J. L.: 1994, *Astron. Astrophys.* **290**, 983.  
Cowling, T. G.: 1945, *Monthly Notices Royal Astron. Soc.* **105**, 167.  
Eddy, J. A.: 1976, *Solar Phys.* **192**, 1189.  
Frick, P., Galyagin, D., Hoyt, D., Nesme-Ribes, E., and Schatten, K.: 1997, *Astron. Astrophys.* **328**, 670.  
Gnevyshev, M. N. and Ohl, A. I.: 1948, *Astron. Zh.* **25**, 18.  
Hoyt, D. V. and Schatten, K. H.: 1996, *Solar Phys.* **165**, 181.  
Hoyt, D. V. and Schatten, K. H.: 1998, *Solar Phys.* **181**, 491.

- Letfus, V.: 1999, *Solar Phys.* **184**, 201.
- Levy, E. H. and Boyer, D.: 1982, *Astrophys. J.* **254**, L19.
- Mordvinov, A. V. and Kuklin, G. V.: 1999, *Solar Phys.* **187**, 223.
- Mundt, M. D., Maguire, H. W. B. II, and Chase, R. P.: 1991, *J. Geophys. Res.* **96**, 1705.
- Mursula, K., Usoskin, I. G., and Kovaltsov, G. A.: 2001, *Solar Phys.* **198**, 51.
- Oliver, R. and Ballester, J. L.: 1996, *Solar Phys.* **169**, 215.
- Ostryakov, V. M. and Usoskin, I. G.: 1990, *Solar Phys.* **127**, 405.
- Ostryakov, V. M. and Usoskin, I. G.: 1990a, *Soviet. Tech. Phys. Lett.* **16**, 658.
- Price, C. P., Prichard, D., and Hogenson, E. A.: 1992, *J. Geophys. Res.* **97**, 19113.
- Pudovkin, M. I. and Benevolenskaya, E. E.: 1984, *Soviet Astron.* **28**, 458.
- Ribes, J. C. and Nesme-Ribes, E.: 1993, *Astron. Astrophys.* **276**, 549.
- Rozelot, J. P.: 1995, *Astron. Astrophys.* **297**, L45, 1995.
- Ruzmaikin, A.: 1997, *Astron. Astrophys.* **319**, L13.
- Ruzmaikin, A.: 1998, *Solar Phys.* **181**, 1.
- Schmitt, D., Schüssler, M., and Ferriz-Mas, A.: 1996, *Astron. Astrophys.* **311**, L1.
- Schüssler, M. P., Caligari, P., Ferriz-Mas, A., and Morena-Insertis, M.: 1994, *Astron. Astrophys.* **281**, L69.
- Sokoloff, D. and Nesme-Ribes, E. N.: 1994, *Astron. Astrophys.* **288**, 293.
- Sonett, C. P.: 1982, *Geophys. Res. Lett.* **9**, 1313.
- Sonett, C. P.: 1983, *Nature* **306**, 670.
- Storini, M. and Sykora, J.: 1997, *Solar Phys.* **176**, 417.
- Usoskin, I. G., Mursula, K., and Kovaltsov, G. A.: 2000, *Astron. Astrophys.* **354**, L33.
- Usoskin, I. G., Mursula, K., and Kovaltsov, G. A.: 2001, *J. Geophys. Res.*, in press.
- Vitinsky, Yu. I.: 1965, *Solar Activity Forecasting*, Israel Program for Scientific Translations, Jerusalem.
- Vitinsky, Yu. I., Kopecký, M., and Kuklin, G. V.: 1986, *Statistics of Sunspot-Formation Activity*, Nauka, Moscow.
- Wilson, P. R.: 1994, *Solar and Stellar Activity Cycles*, Cambridge University Press, Cambridge.
- Wilson, R. M.: 1988, *Solar Phys.* **117**, 269.
- Wilson, R. M.: 1998, *Solar Phys.* **182**, 217.
- Zeldovich, Ya. B., Ruzmaikin, A. A., and Sokoloff, D. D.: 1983, *Magnetic Fields in Astrophysics*, Gordon and Breach, New York.